J|A|C|S COMMUNICATIONS

Published on Web 12/19/2008

Synthesis and Spectroscopic Identification of a μ-1,2-Disulfidodinickel Complex

Matthew T. Kieber-Emmons,[†] Katherine M. Van Heuvelen,[‡] Thomas C. Brunold,[‡] and Charles G. Riordan*,[†]

Department of Chemistry and Biochemistry, University of Delaware, Newark, Delaware 19716, and Department of Chemistry, University of Wisconsin—Madison, Madison, Wisconsin 53706

Received October 7, 2008; E-mail: riordan@udel.edu

The reactivity and coordination chemistry of nickel with sulfur containing ligands such as SR^-, SH^-, and S_x^{n-} has been the subject of considerable research efforts.[1] For example, among its many industrial applications, nickel can function as a key activator in hydrodesulfurization of fossil fuel sources.[2] Jones and co-workers have made considerable progress in deducing the mechanistic details of desulfurization in homogeneous model systems by uncovering a wealth of variable structure types including an intriguing terminal nickel sulfide, the existence of which is inferred from reaction kinetics and chemical trapping with nitroxide reagents.[3] To access new nickel−sulfur structural motifs that can be kinetically trapped and examined in detail, we have investigated an alternative preparative pathway, namely, the reaction of nickel(I) precursors with elemental sulfur.[4] An inherent difficulty in the study of such synthetic systems is the tendency of nickel to form binary sulfides. Nonetheless, several dinickel complexes with bridging sulfide ligands have been prepared.[5] To date, the three crystallographically characterized disulfido. (S_2^{2-}) dinickel complexes contain an η^2:η^2 or "side-on" Ni_2S_2 core structure.[4,6] Complementary to these studies, we report herein the preparation and characterization of the first example of a bridging "end-on" disulfide motif of nickel. This complex provides an excellent platform for the spectroscopic evaluation of this core structure type, reactivity investigations aimed at obtaining fundamental insights relevant to small molecule activation, and the development of stoichiometric and catalytic reagents.

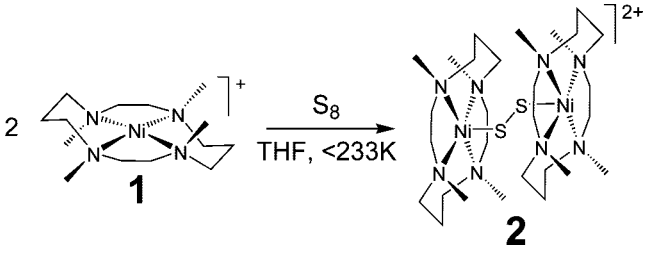

To access new nickel−sulfur structure types, we have employed analogous monovalent nickel precursors as in our recent investigations into dioxygen activation.[7] Specifically, the addition of elemental sulfur to the Ni^{1+} complex [Ni(tmc)](OTf) (**1**, tmc = 1,4,8,11-tetramethyl-1,4,8,11-tetraazacyclotetradecane) at low temperatures immediately yields an intensely purple colored solution. In a typical reaction, sulfur is added dropwise as a solution in THF to a precooled solution of **1**. Strong optical absorption features appear at 647, 529, and 444 nm (ϵ = 2020, 1420, 670 M^{-1} cm^{-1}, THF, 195 K), which are typical for transition metal sulfur adducts.[8,9] Optical titration experiments indicate maximum intensity at 647 nm is achieved at a 1:1 Ni:S stoichiometry (Figure 1). Further addition of another equivalent of sulfur results in a decrease of the band at 647 nm and concomitant growth of the two higher energy features at 529 and 444 nm, which we therefore attribute to a distinct, as yet unidentified species, **3** (Supporting Information (SI)). Room temperature decomposition of **2** is facile yielding an intractable brown solid, presumably nickel sulfide.

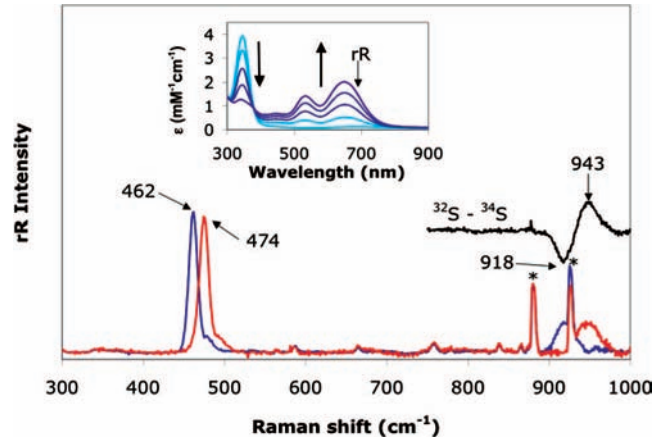

Figure 1. Resonance Raman spectra of **2** (λ_{ex} = 647 nm, 77 K) generated from $^{32}S_8$ (red) and $^{34}S_8$ (blue). Inset: Spectral titration of **1** with [S] yielding a maximum intensity of **2** at 1:1 Ni:S (THF, 195 K).

Resonance Raman spectra obtained with laser excitation into the most intense absorption feature of **2** (excitation λ = 647 nm) exhibit a dominant feature at 474 cm^{-1}, which downshifts to 462 cm^{-1} (Δ = −12 cm^{-1}) in samples prepared with $^{34}S_8$. On the basis of reduced mass calculations, this feature is assigned as a υ(S−S) stretching mode (for an isolated harmonic oscillator: Δ = −14 cm^{-1}). The first overtone of this mode is present at 943 cm^{-1} (^{34}S: 918 cm^{-1}). The rR excitation profile of the 474-cm^{-1} feature mirrors the optical band at 647 nm, suggesting assignment of the band as a S → Ni charge transfer (CT) transition (SI). A weaker intensity vibrational feature at 269 cm^{-1} is tentatively assigned to the υ(Ni−S) mode based on its frequency and isotope sensitivity (Δ = −2.5 cm^{-1}). Excitation at higher energy, specifically into the optical absorption envelope with λ_{max} = 529 nm, results in enhancement of a distinct υ(S−S) feature at 501 cm^{-1} (^{34}S: 488 cm^{-1}), further establishing that this absorption band arises from a different species, **3**. The energy of the υ(S−S) band in **2** compares well to that reported for the crystallographically characterized "end-on" Cu_2S_2 complex $[\{Cu(TMPA)\}_2(\mu\text{-}S_2)]^{2+}$,[10] for which the υ(S−S) mode has been observed at 499 cm^{-1}.[9] In a crystallographically defined $Ni_2(\mu\text{-}\eta^2\text{:}\eta^2\text{-}S_2)$ complex,[8b] the υ(S−S) = 446 cm^{-1} mode is at lower energy consistent with side-on ligation and a weaker S−S bond.[11]

Compound **2** is EPR silent and exhibits paramagnetically shifted spectral features in its ^{1}H NMR spectrum (d_8-THF, 253 K), consistent with an integer spin system and, thus, attributed to a dimer. Observation of two resonances in the ^{2}H NMR spectrum (THF, 253 K) of the

[†] University of Delaware.
[‡] University of Wisconsin−Madison.

10.1021/ja807735a CCC: $40.75

perdeutero-methyl tmc analogue **2-d$_{12}$** is consistent with a square pyramidal stereochemistry. A single paramagnetically shifted feature for unidentified species **3** is also observed in all ^{2}H NMR experiments. Magnetic circular dichroism (MCD) spectra obtained at 4 K indicate **2** is diamagnetic in its ground state (SI). High-resolution electrospray Fourier transform ion cyclotron resonance mass spectrometry (FT-ICR-MS) data of a cold THF solution of **2** support its formulation as a dimer. The most intense feature in the spectrum is attributed to $[Ni(tmc)]^+$. Nonetheless, a low intensity feature is observed with the *m*/*z* ratio and isotopic distribution consistent with the molecular ion, $\{[Ni(tmc)]_2(S_2)][OTf]\}^+$ (*m*/*z* = 841.291949; calcd: 841.291707; Δ = 0.288 ppm; Figure S7).

Preliminary density functional theory (DFT) calculations corroborate the structural assignment of **2** (Figure 2). The structure of the C_{2h} optimized geometry of **2** is characterized by an elongated S−S bond (2.129 Å), compared to that of $[\{Cu(TMPA)\}_2(S_2)]^{2+}$ (2.044 Å).[10] This lengthening is consistent with a weaker S−S bond in the former, and consequently, the lower υ(S−S) vibrational energy observed for **2**. When considering that the primary Ni−S bonding interaction involves the S_2^{2-} π^*_σ and the Ni d_{z^2} orbitals (Figure S8, orbital 186), a weaker S−S bond would indicate a weaker Ni−S interaction. This phenomenon can be understood by appreciating that the extent of Ni−S bonding correlates with removing electron density from the S−S antibonding orbital. Indeed, the DFT-derived Ni−S distance of 2.447 Å, when compared to the Cu−S distance of 2.280 Å in $[\{Cu(TMPA)\}_2(S_2)]^{2+}$, supports this deduction. Time-dependent DFT computations for **2** predict an absorption envelope at 605 nm, in good agreement with the experimentally observed optical transition at 650 nm. Examination of the corresponding electron density difference map indicates transfer of charge from the disulfide to the Ni d_{z^2} orbital and, hence, corroborates assignment of this band to a S → Ni CT transition. DFT analysis further predicts a diamagnetic ground state as observed in the MCD experiments, a consequence of antiferromagnetic coupling (calcd $-2J = 188$ cm^{-1}; $H = -2J\ S_1 \cdot S_2$) between the two Ni^{2+} ions in **2**. Analysis of the variable-temperature ^{2}H NMR spectra of **2-d$_{12}$** leads to $-2J \leq 61$ cm^{-1},[12] in reasonable agreement with the coupling predicted by theory.

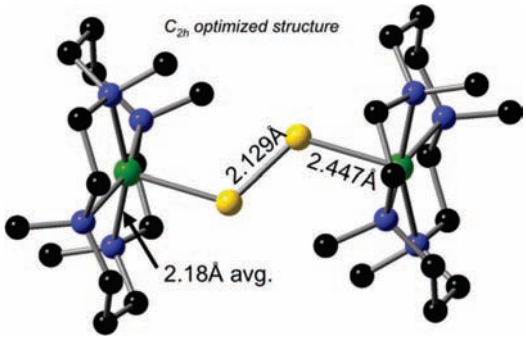

Figure 2. DFT optimized structure of **2** constrained to C_{2h} symmetry, as obtained from a spin-unrestricted B3LYP broken symmetry calculation (M_s = 0) using the B3LYP hybrid functional.

A qualitative comparison between **2** and the isostructural *trans*-1,2-peroxo bridged dinickel complex, $\{[Ni(tmc)]_2(\mu\text{-}O_2)\}^{2+}$ (**4**),[13] is instructive. Because the disulfide π^* orbitals in **2** are higher in energy than the peroxo π^* orbitals in **4**, the former are closer in energy to the nickel 3d orbitals and, thus, interact more strongly to produce more covalent Ni−S bonds in **2** compared to the Ni−O bonds in **4**. However, several other factors, such as differences in the Ni−S−S and Ni−O−O bond angles will presumably also contribute to the differences in quantitative bonding characteristics between **2** and **4**. For **4** it was shown that this species possesses significantly less covalent metal−oxygen bonds than the related copper complex, due to the lower effective nuclear charge of nickel compared to copper, which leads to a decreased stabilization of the nickel 3*d* orbitals and, therefore, to weaker nickel−oxygen bonding interaction.[14] Collectively, the results obtained for these *trans*-μ-1,2-dichalcogenide structures suggest that the Ni−S interaction is stronger than the Ni−O interaction, whereas the Ni−O/S interactions are weaker than the corresponding Cu−O/S interactions. This decreased O/S → Ni charge donation should also enhance the nucleophilic character of the dichalcogenide moiety, which bodes well for future reactivity studies. A more detailed computational/spectroscopic analysis is in progress to generate a quantitative bonding description for this new nickel structure type.

In summary, we have spectroscopically identified a *trans*-μ-1,2-disulfido complex of nickel (**2**) as evidenced by NMR, ESI-MS, resonance Raman, MCD, and UV−vis spectral titration measurements. DFT computational studies support this proposed core structure for **2** and reveal rather long Ni−S and S−S bonds. This prediction is consistent with the observation that **2** is thermally unstable, in stark contrast to (μ-η^2:η^2) disulfidodinickel complexes. This complex, which represents the first example of an "end-on" disulfido motif in nickel coordination chemistry, provides an excellent platform for further investigations into the mechanism of small molecule activation by nickel complexes.

Acknowledgment. Support from the National Science Foundation (CHE-0518508 and CHE-0809603) to C.G.R. and the NSF Graduate Research Fellowship Program to K.M.V.H. is greatly appreciated. Some of the computational resources used in these studies were provided by the INBRE supported Bioinformatics Center of the University of Arkansas for Medical Sciences (NIH P20 RR-16460).

Supporting Information Available: Experimental details, characterization data, and computational methods. This material is available free of charge via the Internet at http://pubs.acs.org.

References

(1) *Transition Metal Sulfur Chemistry: Biological and Industrial Significance*; ACS Symposium Series 635; American Chemical Society: Washington, DC, 1996.
(2) Kabe, T. *Hydrodesulfurization and hydrodenitrogenation: chemistry and engineering*; Wiley-VCH: New York, 1999.
(3) Vicic, D. A.; Jones, W. D. *J. Am. Chem. Soc.* **1999**, *121*, 4070–4071. Vicic, D. A.; Jones, W. D. *J. Am. Chem. Soc.* **1999**, *121*, 7606–7617.
(4) Cho, J.; Heuvelen, K. M. V.; Yap, G. P. A.; Brunold, T. C.; Riordan, C. G. *Inorg. Chem.* **2008**, *47*, 3931–3933.
(5) (a) Mealli, C.; Midollini, S.; Sacconi, L. *Inorg. Chem.* **1978**, *17*, 632–637. (b) Oster, S. S.; Lachicotte, R. J.; Jones, W. D. *Inorg. Chim. Acta* **2002**, *330*, 118–127.
(6) (a) Mealli, C.; Midollini, S. *Inorg. Chem.* **1983**, *22*, 2786–2787. (b) Pleus, R. J.; Waden, H.; Saak, W.; Haase, D.; Pohl, S. *J. Chem. Soc., Dalton Trans.* **1999**, 2601–2610.
(7) Kieber-Emmons, M. T.; Riordan, C. G. *Acc. Chem. Res.* **2007**, *40*, 618–625.
(8) (a) Sellmann, D.; Lechner, P.; Knoch, F.; Moll, M. *J. Am. Chem. Soc.* **1992**, *114*, 922–930. (b) Franolic, J. D.; Millar, M.; Koch, S. A. *Inorg. Chem.* **1995**, *34*, 1981–1982.
(9) Chen, P.; Fujisawa, K.; Helton, M. E.; Karlin, K. D.; Solomon, E. I. *J. Am. Chem. Soc.* **2003**, *125*, 6394–6408.
(10) Helton, M. E.; Chen, P.; Paul, P. P.; Tyeklar, Z.; Sommer, R. D.; Zakharov, L. N.; Rheingold, A. L.; Solomon, E. I.; Karlin, K. D. *J. Am. Chem. Soc.* **2003**, *125*, 1160–1161.
(11) Brown, E. C.; Bar-Nahum, I.; York, J. T.; Aboelella, N. W.; Tolman, W. B. *Inorg. Chem.* **2007**, *46*, 486–496.
(12) As shown in the Supporting Information, a fit of the VT ^{2}H NMR spectral data to the effective Hamiltonian that leads to this coupling constant is not statistically better than a fit to a simple Curie paramagnet. However, given the $S = 0$ ground state determined by MCD measurements and the lack of an EPR signal, we put forth an antiferromagnetically coupled dimer as the appropriate model for **2**.
(13) Kieber-Emmons, M. T.; Schenker, R.; Yap, G. P. A.; Brunold, T. C.; Riordan, C. G. *Angew. Chem., Int. Ed.* **2004**, *43*, 6716–6718.
(14) Schenker, R.; Kieber-Emmons, M. T.; Riordan, C. G.; Brunold, T. C. *Inorg. Chem.* **2005**, *44*, 1752–1762.

JA807735A